Angewandte Chemie
Eine Zeitschrift der Gesellschaft Deutscher Chemiker

Supporting Information

69451 Weinheim, Germany

Proton-Detected Solid-State NMR Spectroscopy of Fibrillar and Membrane Proteins**

Rasmus Linser, Muralidhar Dasari, Matthias Hiller, Victoria Higman, Uwe Fink, Juan-Miguel Lopez del Amo, Stefan Markovic, Liselotte Handel, Brigitte Kessler, Peter Schmieder, Dieter Oesterhelt, Hartmut Oschkinat, and Bernd Reif**

anie_201008244_sm_miscellaneous_information.pdf

Supplementary Information

I. NMR-Spectroscopy

2D H/N-correlations were recorded using CP-based experiments (Supporting Figure 1A). After the constant-time ^{15}N evolution period, water suppression was achieved with four successive 15 ms purge pulses (ω_{rf} = 10 kHz) with alternating phases according to Zhou et al.[1] Magnetization transfer was achieved via ramp-CP. For OmpG and Aß$^{1-40}$, CP yields better sensitivity in comparison to experiments in which INEPT steps are employed for magnetization transfer. For bR, INEPT based sequences yield a better signal-to-noise ratio. Phase-sensitive detection in the indirect dimension was conducted according to States-TPPI. For assignment, out-and-back triple resonance experiments[2, 3] were employed (Supporting Figure 1B and 1C). Optimal sensitivity was achieved when dipolar ^{1}H,^{15}N and scalar ^{15}N,^{13}C transfer steps were implemented. Long purge pulses were again employed for water suppression.[1] On- and off-resonance ^{13}C pulses were applied as soft rectangular and G3 shaped pulses, respectively.[4, 5]

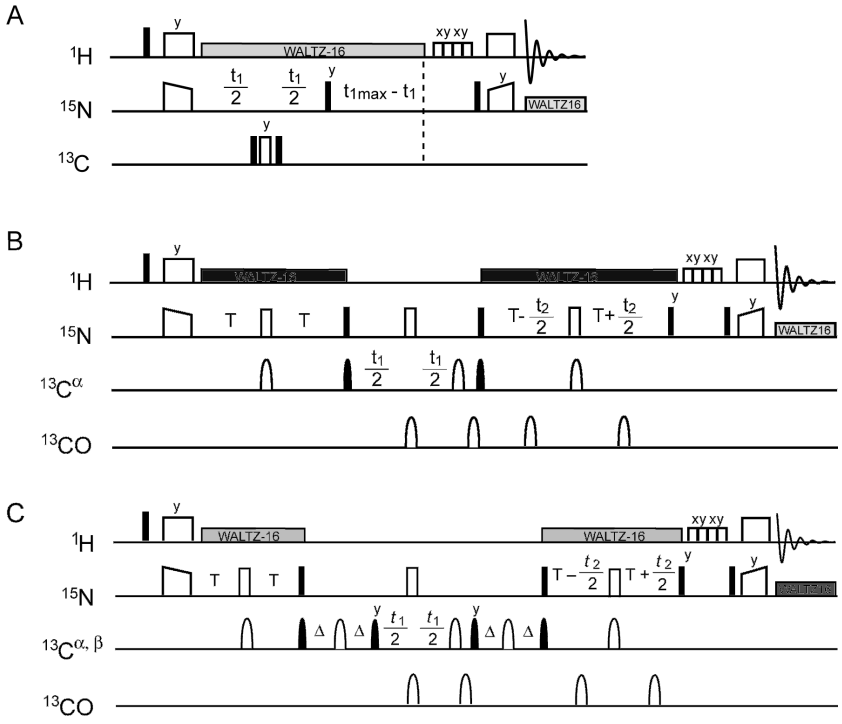

Supporting Figure 1. Proton detected NMR experiments. **A)** 2D H/N-correlation based on the MISSISSIPPI pulse scheme proposed by Zhou et al.[1] **B)** HNCA. CP is employed for magnetization transfer between ^{1}H and ^{15}N. Water suppression was again achieved using long purge pulses.[1] **C)** HNCACB. t, T, and ? were set to 2.3, 12.0, and 3.6 ms, respectively. Decoupling during acquisition was carried out using WALTZ-16,[6] adjusting the ^{15}N RF field

to 2 kHz. In the HNCA, the ^{13}C carrier was set on-resonance to C^{a} frequencies, using a spectral width of 40 ppm. In the HNCACB, the ^{13}C carrier was centered between C^{a} and $C^{ß}$, employing a spectral width of 70 ppm. The maximum ^{13}C acquisition time t_1^{max} amounted to 10 and 6 ms in the HNCA and the HNCACB experiments, respectively.

2. Alzheimer's disease Aß$^{1-40}$ fibrils

Expression of uniformly [^{2}D, ^{15}N, ^{13}C]-labeled Aß$^{1-40}$ was achieved by recombinant expression in *E.coli* (BL21 DE3), using a p28a vector (Novagen) carrying an insert encoding for the Aß$^{1-40}$ sequence. Expression tests were performed in LB, subsequent expression of labelled protein was carried out in isotopically enriched M9 medium (0.5 g/l $^{15}NH_4Cl$, 2 g/l ^{13}C glucose) containing 50 mg/l kanamycin. Cell cultures were grown to an OD_{600} of 0.6 at 37 °C and induced using 1 mM IPTG. The cells were harvested after 4 h by centrifugation, the pellet was resuspended and lysed by sonication. Inclusion bodies were purified using a differential centrifugation-detergent wash procedure[7, 8] with repeated washing steps (resuspension of the pellet by sonication and centrifugation) in a buffer containing 50 mM Tris-HCl pH 7.5, 100 mM NaCl, 1 mM EDTA, 0.1 % NaN_3, and 0.5 % triton X-100. In order to obtain a monomeric peptide solution, we employed the protocols developed by Teplow,[9] and Hou et al.[10] with minor modifications. In brief, the peptide was dissolved in 20 mM NaOH, sonicated and passed through a filter (0.22 µm pore size). The peptide solution was diluted into Tris-buffer (pH 7.2) (final concentration of Aß$^{1-40}$: 150 µM), seeded with preformed sonicated fibrils (12 generations of seeding), and incubated at room temperature under agitation for one week. The buffer contained H_2O and D_2O at mixing ratios of H_2O/D_2O = 0.1, 0.25, 0.30 or 0.5. To exploit PRE (Paramagnetic Relaxation Enhancement), Cu(edta) was added to the monomeric Aß$^{1-40}$ peptide, prior to fibrilization using concentrations of 75 or 100 mM of Cu(edta). Growth and quality of the fibrils was monitored by EM. For each sample, typically 10 mg of Aß$^{1-40}$ fibrils were packed into a 3.2mm MAS solid-state NMR rotor.

In order to find out if Cu(edta) has an effect on the NMR spectral quality, H/N correlation spectra of Aß$^{1-40}$ fibril samples were recorded in the presence and absence of the metal chelate (Supporting Figure 2A and 2B). The amyloid fibril morphology as judged by electron microscopy is unchanged independent of Cu(edta) (data not shown). Also, the overall spectral appearance is very similar. In particular, the resolution is not compromised if Cu(edta) is

added to the fibril preparation. In the absence of the metal chelate, the achievable sensitivity is, however, reduced. The ^{1}H-T_1 relaxation times of samples with Cu(edta) amount to 0.13-0.18 s, whereas we obtain a value of (1.53 +/- 0.01) s in the absence of Cu(edta). Supporting Figure 2C and 2D show the effect of seeding on the quality of the 2D H/N correlation spectra. Clearly, the number of cross peaks is increased in cases where no seeds are added prior to fibril formation. However, the resolution is comparable in both cases, indicating that seeding does not determine the achievable resolution in the spectra. To probe the influence of protonated buffers, the sample that was used to record the spectrum shown in Supporting Figure 2E was prepared using 25 mM phosphate buffer instead of Tris. Supporting Figure 2F shows a preparation in which 50% H_2O was employed in the buffer for fibril formation. The resolution in the ^{1}H and ^{15}N dimension of these spectra is comparable to the other preparations. We therefore assume that the achievable resolution is not determined by residual ^{1}H,^{1}H dipolar interactions. This is in agreement to what has been found previously for a microcrystalline preparation of the α-spectrin SH3 domain.[11]

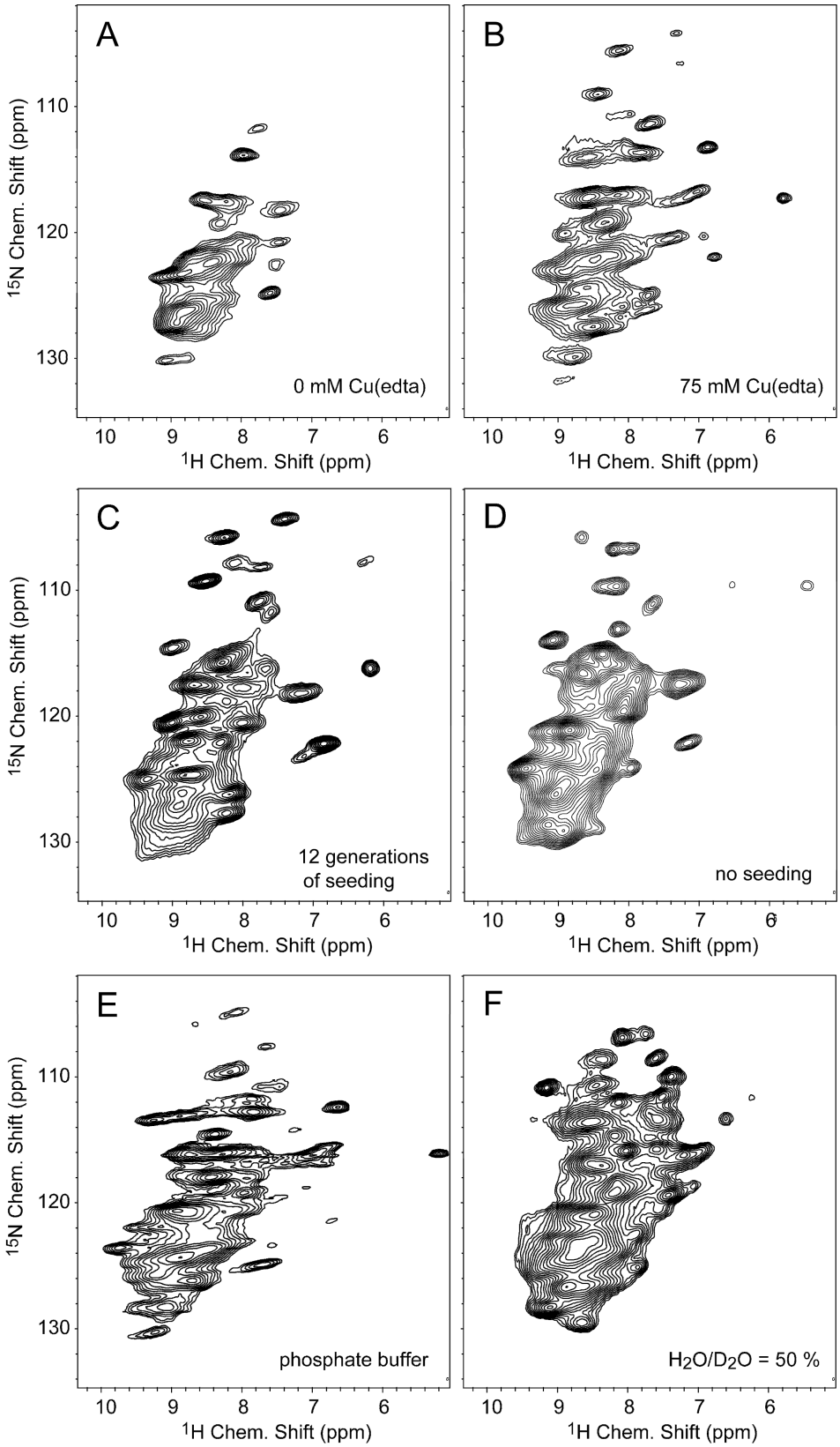

Supporting Figure 2. A and **B)** Comparison of H/N correlation spectra of Aß$^{1-40}$ fibrils prepared without and with of 75 mM Cu(edta), respectively. The absence of weaker cross peaks in A is due to the long T_1, resulting in low sensitivity even after an experimental time of 14 h. **C)** and **D)** Comparison of H/N correlation spectra of Aß$^{1-40}$ fibrils with and without seeding. The spectrum in **E)** was recorded for an Aß$^{1-40}$ sample that was solubilized in

phosphate (25 mM) instead of Tris buffer. **F)** H/N correlation spectrum of an Aß$^{1-40}$ fibril preparation obtained from a buffer containing 50 % instead of 25% H_2O. All spectra were recorded using the pulse scheme shown in Supporting Figure 1A.

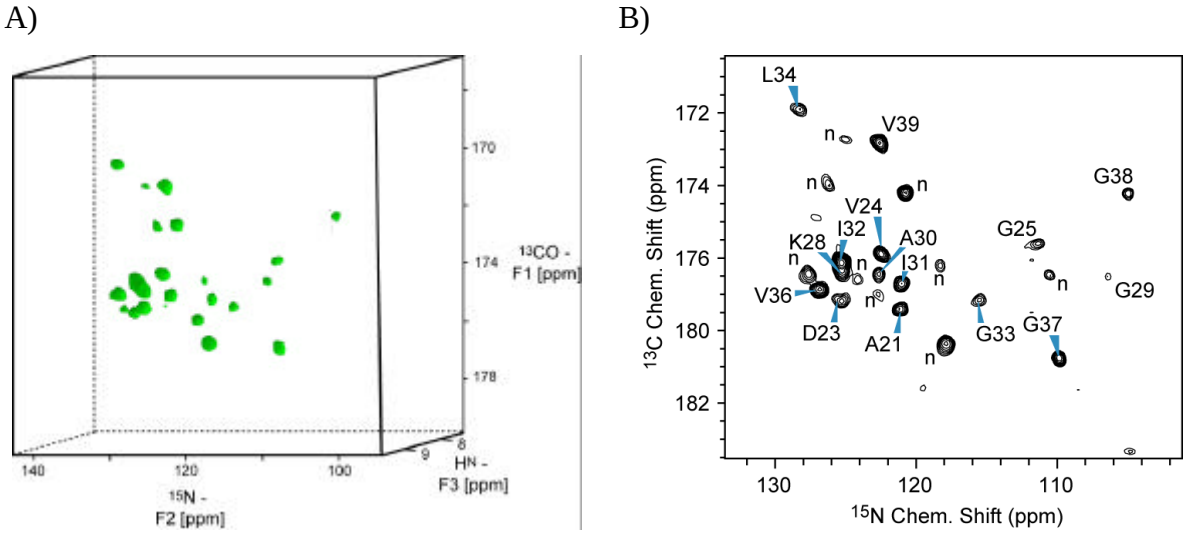

Supporting Figure 3. A) 3D cube representation of the 3D HNCO experiment recorded for Aß$^{1-40}$ fibrils. **B)** ^{15}N/^{13}C projection of the 3D HNCO experiment. The spectrum was recorded using an INEPT based experiment.[5] The experimental time amounted to 2.5 d. A t_2^{max} of 20 ms and 22 ms t_1^{max} were used in the indirect ^{15}N and ^{13}CO dimension, respectively. Time domain data were processed employing Gaussian apodization using -10 Hz line broadening and a shift of the bell by 0.1. Linewidths in the carbonyl dimension amount to ca. 50-60 Hz.

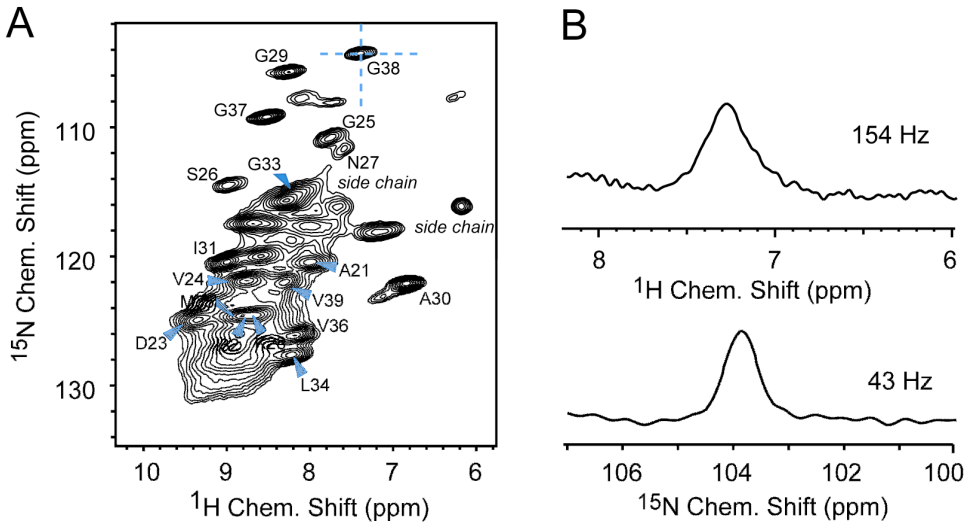

Supporting Figure 4. A) 2D H/N correlation of Aß$^{1-40}$ fibrils. **B)** Cross sections along the ^{15}N and ^{1}H dimension.

In order to test if ns-µs timescale motion is the source of the residual $^{1}H/^{15}N$ line width, we carried out ^{15}N-Hα/^{15}N-Hβ spin state selective experiments (Supporting Figure 5). We found that TROSY-type experiments do not yield an increase in spectral resolution. As a consequence, this indicates that either static disorder or slow exchange dynamics is the primary source for ^{1}H and ^{15}N line broadening.

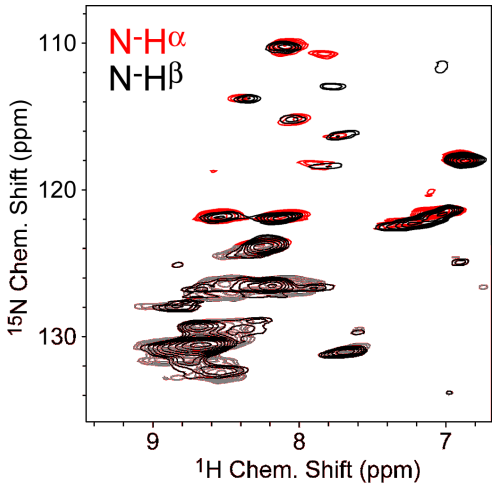

Supporting Figure 5. Comparison of 2D H/N correlation spectra selecting the ^{15}N-Hα (red) and ^{15}N-Hβ spin-states in a Aß$^{1-40}$ fibril sample. No significant differences are observed, indicating that no large amplitude ns-µs timescale motion occurs.[12] The experiments were recorded at 900 MHz within 3 h, employing t_1^{max} = 30 ms. The MAS rotation frequency was adjusted to 20 kHz. The effective sample temperature was 20°C.

3. Bacteriorhodopsin (bR)

u-(^{2}H, ^{15}N, ^{13}C)-labelled purple membrane was obtained as described previously.[13, 14] Partial deuterium-proton exchange at labile sites was achieved by resuspension of the membranes in a buffer containing H_2O and D_2O at a ratio of 10 % at pH 9.5. After one week of incubation, the membranes were centrifuged and resuspended in buffer at pH 7. After incubation for another 2 h, ca. 10 mg of material was filled into a 3.2mm MAS rotor.

4. Outer Membrane Protein G (OmpG)

OmpG was prepared as described by Hiller *et al.*[15] In order to obtain a deuterated sample, the protein was expressed as inclusion bodies using fully deuterated M9 minimal medium containing u-[^{2}H,^{13}C]-glucose and ^{15}N-NH_4Cl as sole carbon and nitrogen sources, respectively. After purification under denaturing conditions (8M urea), the proton content of

the backbone amide was set to 30 % by multiple buffer exchange steps (Supporting Figure 6A). Native OmpG was obtained by refolding the protein in a detergent containing buffer. For this purpose, a 1 mM solution from lyophilised dodecyl-β-D-maltoside was prepared using the refolding buffer (30% H_2O and 70% D_2O). Similarly, the buffer for the subsequent reconstitution and 2D crystallisation also contained 30 % H_2O and 70 % D_2O.

A)

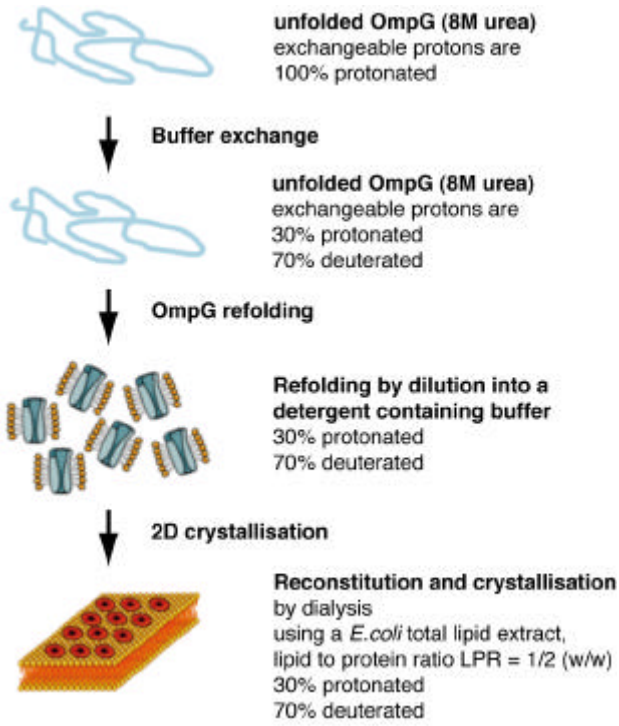

B)

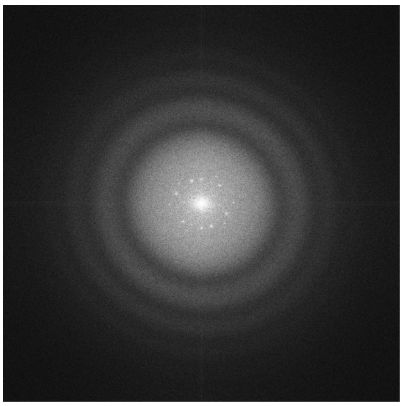

C)

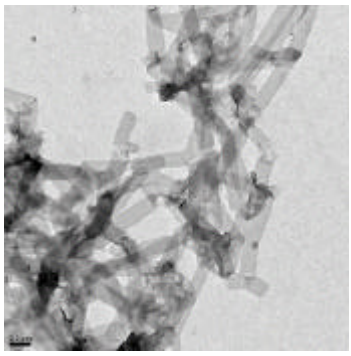

D)

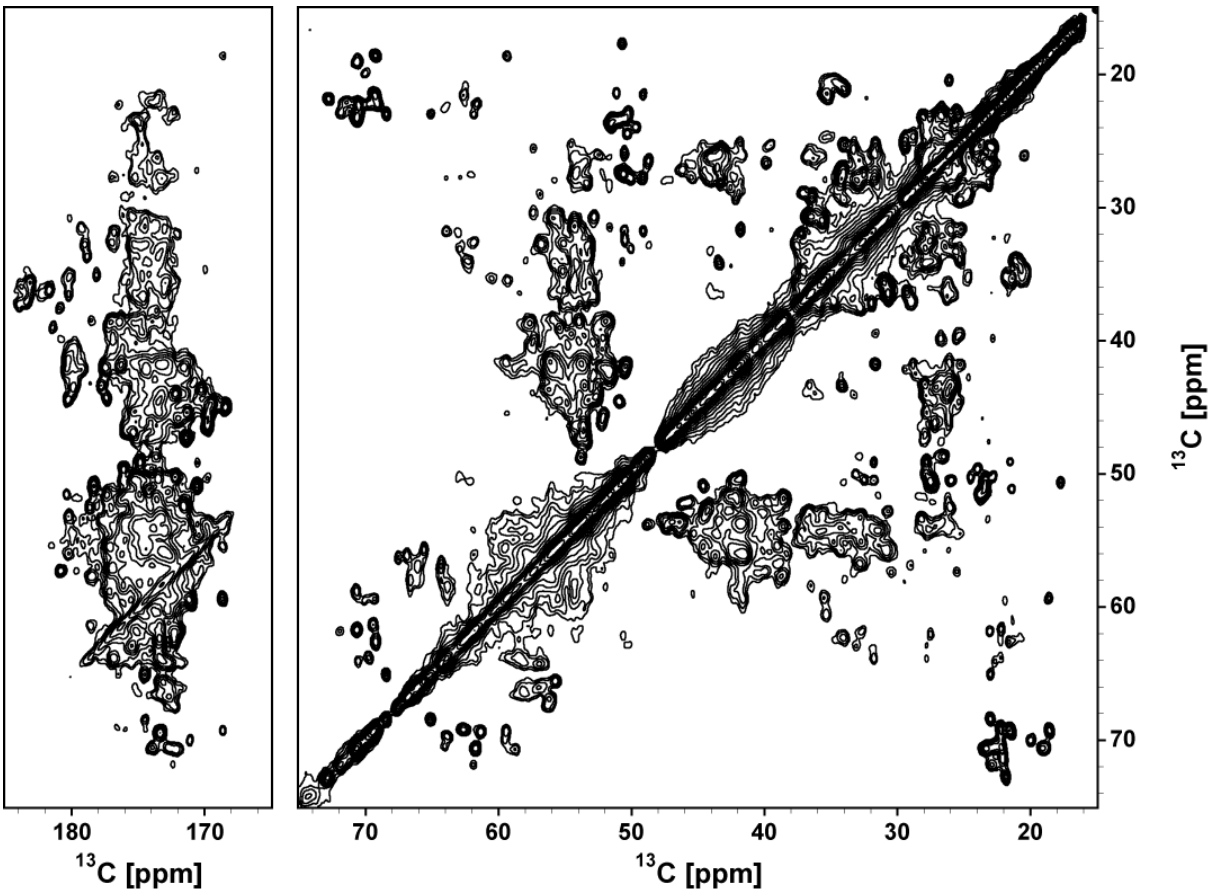

Supporting Figure 6. A) Preparation of partially protonated ^{13}C, ^{15}N labelled OmpG. **B)** X-ray diffraction pattern of OmpG 2D crystals. A reduced long-range order of these crystals results in a low resolution diffraction pattern. For solid-state NMR, however, short range order is sufficient to obtain well resolved spectra. **C)** Electron micrograph of 2D OmpG crystals reconstituted in lipid bilayers. **D)** 2D-^{13}C, ^{13}C correlation spectrum of lipid reconstituted OmpG, using 25 ms of proton driven spin diffusion (PDSD) for ^{13}C,^{13}C mixing.

The obtained crystals have a tubular shape, and are up to 1µm in length and approximately 180 nm in width (Supporting Figure 6A and 6C). From these crystals, a projection structure with 6 Å resolution could be calculated.[16] Subjecting the 2D crystals to X-ray analysis resulted in a diffraction pattern of relatively low quality (see Supporting Figure 6B). Short range order is, however, sufficient to obtain well resolved MAS solid-state NMR spectra (Supporting Figure 6D). 2D H/N-correlation spectra of OmpG preparations with protonated and deuterated *E. coli* lipids, acquired at 850 MHz, are shown in Supporting Figure 7. In both experiments, the MAS rotation frequency was adjusted to 20 kHz. The temperature in the experiments was set to 7 °C. We find comparable spectral resolution for the two preparations. Differences in chemical shifts are observed for a few amide resonances, which is presumably due to a slightly different lipid composition in the two preparations. The relaxation properties of the two preparations are tabulated in Table 1 of the main manuscript.

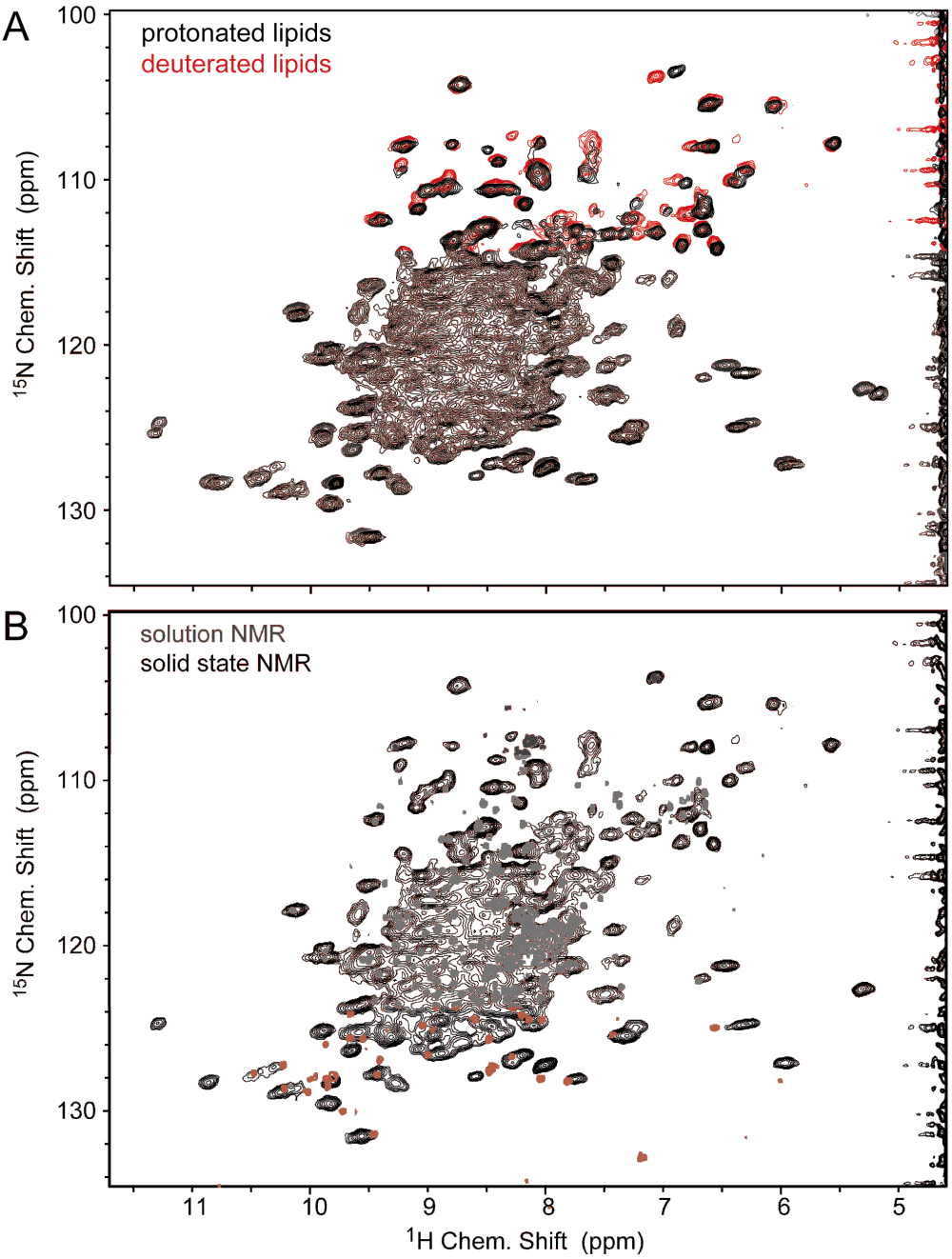

Supporting Figure 7. A) H/N-correlation spectra of OmpG reconstituted in protonated (black) and deuterated (red) *E.coli* lipid extracts. Spectra were acquired at 850 MHz and at a MAS rotation frequency of 20 kHz. The effective sample temperature was set to 25 °C. **B)** Superposition of the H/N-correlation spectra obtained in the solid state (black) and in solution (red). The solution-state spectrum was recorded using a TROSY experiment at 900 MHz, setting the temperature to 27 °C. For the solution-state NMR experiments, the protein was solubilized in dodecyl-β-D-maltoside.

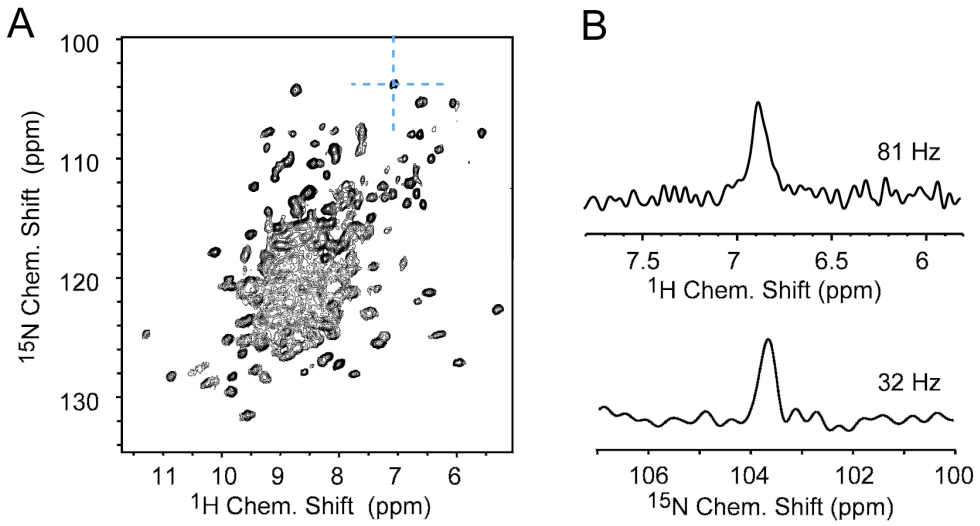

Supporting Figure 8. A) 2D H/N correlation of OmpG. **B)** Cross sections along the ^{15}N and ^{1}H dimension. The spectra refer to the sample containing deuterated *E.coli* lipid extracts.

References

[1] D. H. Zhou, C. M. Rienstra, *J. Magn. Reson.* **2008**, *192*, 167–172.
[2] S. Grzesiek, A. Bax, *J. Magn. Reson.* **1992**, *189*, 432.
[3] M. Wittekind, L. A. Mueller, *J. Magn. Reson. B* **1993**, *101*, 201.
[4] L. Emsley, G. Bodenhausen, *Chem. Phys. Lett.* **1990**, *165*, 469.
[5] R. Linser, U. Fink, B. Reif, *J. Magn. Reson.* **2008**, *193*, 89–93.
[6] A. J. Shaka, J. Keeler, T. Frenkiel, R. Freeman, *J. Magn. Reson.* **1983**, *52*, 335.
[7] M. Carrio, N. Gonzalez-Montalban, A. Vera, A. Villaverde, S. Ventura, *J. Mol. Biol.* **2005**, *347*, 1025.
[8] L. Wang, S. K. Maji, M. R. Sawaya, D. Eisenberg, R. Riek, *PLoS Biol.* **2008**, *6*, e195.
[9] D. B. Teplow, *Methods Enzymol.* **2006**, *413*, 20.
[10] L. Hou, I. Kang, R. E. Marchant, M. G. Zagorski, *J. Biol. Chem.* **2002**, *277*, 40173.
[11] Ü. Akbey, S. Lange, T. W. Franks, R. Linser, A. Diehl, B. J. van Rossum, B. Reif, H. Oschkinat, *J. Biomol. NMR* **2010**, *46*, 67–73.
[12] R. Linser, U. Fink, B. Reif, *J. Am. Chem. Soc.* **2010**, *132*, 8891–8893.
[13] D. Oesterhelt, W. Stoeckenius, *Methods Enzymol.* **1974**, *31*, 667.
[14] H. Patzelt, A. S. Ulrich, H. Egbringhoff, P. Dux, J. Ashurst, B. Simon, H. Oschkinat, D. Oesterhelt, *J. Biomol. NMR* **1997**, *10*, 95.
[15] M. Hiller, L. Krabben, K. R. Vinothkumar, F. Castellani, B. Van Rossum, W. Kühlbrandt, H. Oschkinat, *ChemBioChem.* **2005**, *6*, 1679.
[16] M. Behlau, D. J. Mills, H. Quader, W. Kuhlbrandt, J. Vonck, *J. Mol. Biol.* **2001**, *305*, 71.